JTTEE5 20:744–759
DOI: 10.1007/s11666-011-9642-0
1059-9630/$19.00 © ASM International

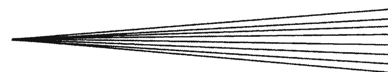

Peer Reviewed

Nonequilibrium Atmospheric Plasma Deposition

T. Belmonte, G. Henrion, and T. Gries

(Submitted December 23, 2010; in revised form February 21, 2011)

This study is a review of plasma enhanced chemical vapor deposition (PECVD) at atmospheric pressure. Sources for coatings over large area are presented. Millimetric torches and microplasmas are next studied for localized PECVD. A specific attention is paid to the way power is dissipated and the consequences it has on the deposition rate and on quality of thin films.

Keywords afterglow, APGD, atmospheric pressure, DBD, microwave, PACVD, PECVD, post-discharge, remote plasma, resonant cavity

1. Introduction

Thermally assisted deposition at atmospheric pressure has been studied intensively during the 1970s and 1980s where there was an urgent need to deposit epi-silicon (Ref 1-7). Many basic works (Ref 8-13) showed the importance of controlling the gas hydrodynamics whose complexity, especially in terms of instability (Ref 12, 13), required strong numerical efforts to be accurately described by computational fluid dynamics. Special efforts were also carried out to determine the reaction mechanisms at the origin of thin film deposition (Ref 14-16).

Resorting to nonequilibrium media like those commonly produced by plasma assistance offers several advantages among which one finds two important features: first, the possibility to deposit thin films down to room temperature (Ref 17); second—and this aspect has recently been emphasized (Ref 18-21)—the possibility to nanostructure surfaces by submitting a surface to extremely nonequilibrium media. What is meant here by "extremely" nonequilibrium is a huge difference in the characteristic plasma temperatures and steep gradients in temperature and density. This scope has been found out only recently, likely because remote plasmas, rather than direct plasma processes, have been more specifically studied (Ref 22-26). The spatial separation between the discharge generation region and the deposition area, thus reducing the possibility of bombardment of the growing film by plasma species provides a better control of the layer growth (Ref 27). Generally, the less stable compounds are introduced downstream from the discharge, what simplifies considerably the chemical pathways, leading to less interdependence of process parameters (Ref 22).

When pressure is raised up to one atmosphere, other basic difficulties arise together with technological drawbacks due to the choice of handling large plasmas or sets of individual sources. Atmospheric pressure plasma enhanced chemical vapor deposition AP-PECVD has the following liabilities:

- laminar diffusion is extremely limited,
- chemical pathways are totally unexplored,
- cluster and powder formation only starts being studied (Ref 28-32).

Technologically:

- powder synthesis is the major difficulty to cope with (Ref 33),
- gas contamination is extremely easy on industrial process lines, due to the greater gas density and residence times. Construction of reactor chamber is sometimes required, eliminating many of the purported advantages of AP-CVD (Ref 34),
- large plasma sources like DBD require elevated power supplies and arcing may occur, large dielectrics and accurate inter-electrode spacing (Ref 35),
- juxtaposition of individual sources over large surfaces creates overlapping areas which have to be managed to achieve satisfying homogeneity in thickness of the deposited layers (Ref 36).

On the one hand, the following advantages are sought:

- extremely fast deposition rates, compliant with continuous flow processes operated at high speed (Ref 22, 23),
- no vacuum system, making them relatively low cost and easy to implement on already existing production lines,
- high versatility of plasma sources that can be utilized to clean surface prior to deposition (Ref 37),
- amazing capabilities to grow patterned or nanostructured surfaces (Ref 38).

T. Belmonte, G. Henrion, and **T. Gries**, Department of Physics and Chemistry of Solids and Surfaces, Institut Jean Lamour, Nancy-Université, CNRS, Parc de Saurupt, CS 14234, 54042 Nancy Cedex, France. Contact e-mails: thierry.belmonte@mines.inpl-nancy.fr and thierry.belmonte@ijl.nancy-universite.fr.

The advent of microplasmas over the last 10 years made also ''localized'' deposition possible (Ref 39-45). Deposition, as usually understood in CVD, normally produces thin films in two dimensions, the third one being their thickness which is very much smaller. It becomes localized when the dimensionality of the deposited coating is zero dimensional, i.e., a dot on the surface of a substrate (Ref 46-48). Reducing dimensions led to micro-CVD, i.e., deposition area below 1 mm^2. By moving the plasma source, threads and more complicated objects can be built. Up to now, the characteristic dimensions of microplasmas remain above a few tens of micrometers (Ref 40-45, 49, 50).

We review the most important results obtained in the field of nonequilibrium atmospheric plasma deposition. The specific case of carbon nanotubes will not be included in this study, a review being already available on this topic (Ref 51). The outline of the study is as follows. In a first step, we shall describe the influence of the choice of a plasma source on deposition. In a second step, we shall show the influence of reducing the size of the plasma source on deposition.

2. Influence of Plasma Sources on Deposition

Because it seems rather simple to scale-up AP-PECVD on roll-to-roll processes, there is a strong industrial demand to bring to flat products new surface functionalities. One practical aspect deals with the distance between the plasma and the substrate to be treated. The closest is usually the best, limiting residence time and then, powder synthesis and depletion of active species. This distance must not be much higher than 10 mm. If the oscillation of the substrate on the line cannot be suppressed by stretchers, like in the case of thick metallic foils, the variation of the plasma-substrate distance may be detrimental to the coating quality. In dielectric barrier discharges, this distance is simply the inter-electrode gap distance. This kind of low temperature source is particularly adapted to the treatment of thin foils of polymers (Ref 22), although the filamentary structure of these plasmas may cause surface damages. Alternatives were proposed to circumvent this difficulty like direct (Ref 52) or remote DBD (Ref 22). Up to now, deposition rates with DBD sources remain relatively low (typically below 10 μm/h). It is basically due to the low power densities usually dissipated in these sources (~a few W/cm^3). It is also a condition to fulfil to keep a low temperature of the neutral species. Increasing the power densities* up to several tens of W/cm^2 enables higher deposition rates (typically below 300 μm/h, Ref 23). Arcs and microwave plasmas are the most widely used sources to work at high power densities. Example of these low (typically below 10 W per cm^2 of coated area) and high (typically above 10 W per cm^2 of coated area) power sources is depicted in Fig. 1.

2.1 Low Power Sources

Dielectric Barrier Discharges are interesting sources to coat substrates at atmospheric pressure, since they are relatively simple to build and to scale up. In Table 1, we list a set of works (Ref 53-72) showing the various possibilities investigated to deposit thin films by low power sources. The common operational mode of atmospheric pressure DBD is filamentary (Ref 54, 57-67, 71), resulting in strong spatial nonuniformity of plasma chemistry that can alter the quality of the films. On the contrary, glow DBD modes (Ref 53, 55, 56, 68-70, 72), sometimes, referred to as low current atmospheric pressure Townsend-like discharge or high current atmospheric pressure glow-like discharge, are expected to give high quality films. This uniform mode of DBD is observed for a very restricted set of parameters such as gas mixture, dissipated power, operational frequency, etc. Consequently, the introduction of a large amount of precursor, e.g., to increase deposition rate, affects the stability of the discharge and turns it into a filamentary one.

From Table 1, we notice several important aspects:

- glow mode leads to higher deposition rates at similar powers per coated area unit,
- deposited power per coated area unit remains small (below 10 W/cm^2),
- deposition rates are always below 10 μm/h in filamentary mode,
- deposition rates in glow mode are usually higher and can reach, at least in one case (Ref 55, 56), extremely high values (several mm/h).

In Fig. 2, the deposition rate is plotted as a function of the power per coated area unit for examples given in Table 1. We clearly observe that there is no straight correlation between these parameters in the case of filamentary discharges. It would also be easy to show that deposition rate and power per plasma volume are not correlated neither. On the contrary, such a correlation seems (because the number of points is restricted) to be valid in the case of glow discharges. Rigorously, the dependence on the partial pressures of active species should also be taken into account, except if surface processes are limiting. Since temperatures are close to room temperature in each case, this dependence may become negligible due to fast transport processes in the gas phase (see for instance Ref 61). Precursors being very different in this set of experiments, this linear dependence would result, for instance, from desorption of similar by-products like carbonaceous species.

Therefore, we can assume that one of the main difference between filamentary and glow discharge is the transport of species to the substrate, although no formal evidence can be provided. However, some elements

*We choose to present results in terms of power dissipated to coat an area unit. This concept is more adapted to the present purpose than the power dissipated by plasma volume unit, more generally encountered. When it is divided by the deposition rate, it gives the energy needed to coat a substrate per volume area of deposited coating.

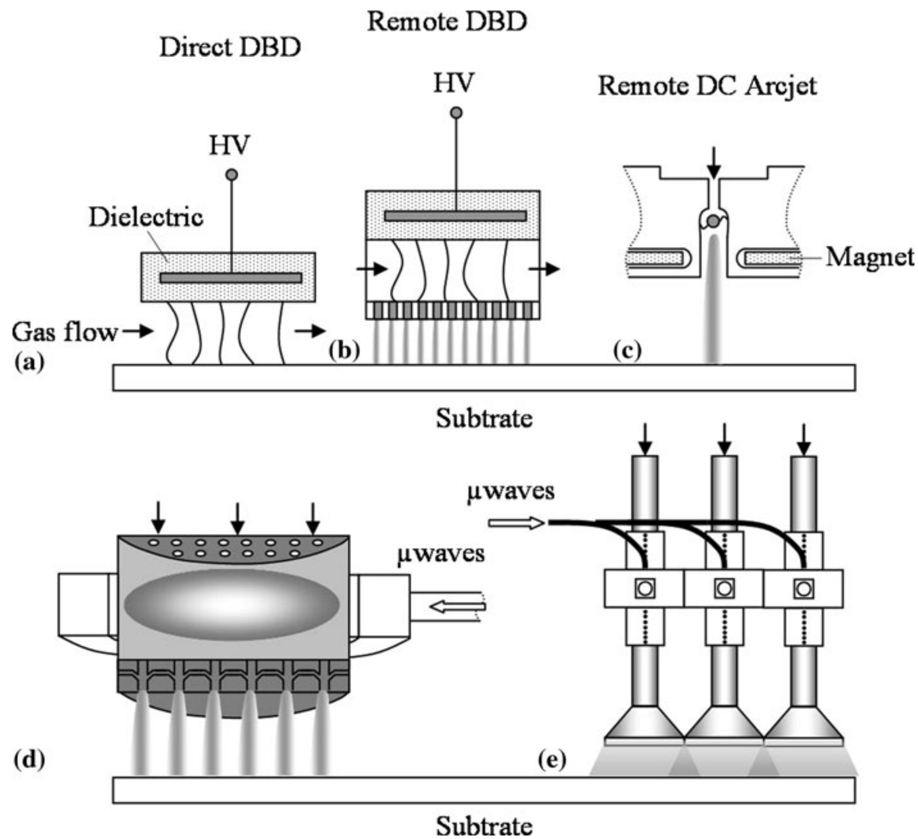

Fig. 1 Example of atmospheric pressure PECVD processes. Up: large plasma sources. (a) Conventional DBD (e.g., Ref. 53), (b) Remote DBD (e.g., Ref 22), and (c) Linear extended DC ArcJet (e.g., Ref 23). Down: individual plasma sources. (d) Microwave remote plasma with slot antenna (e.g., Ref 24) and (e) Remote resonant cavity plasma (e.g., Ref 26)

support this assertion. For instance, Premkumar et al. (Ref 72) succeeded recently in depositing films with a roughness comparable to initial substrate roughness, as in an epitaxial growth. According to these authors, the uniform film deposition would be due to the plasma uniformity at the time scale defined by the time it takes for radicals produced in the gaseous gap to diffuse to the substrate surface. If this step would be limiting, the roughness would change versus the distance in the flow direction due to the depletion of active species, the consequent decrease in the strength of the diffusion flux, and the increase in the time scale. Now, if we rather assume that desorption is limiting, we can expect to keep the same surface roughness as long as the depletion of the precursor in the gas phase does not affect radical adsorption, i.e., as long as active species are sufficiently concentrated to saturate the surface.

In Table 1, we notice that the group of Osaka (Ref 55, 56) obtained deposition rates two orders of magnitude higher than those of all other groups. These authors suggest that the conditions to fulfil to get high deposition rates are the following ones:

- cool the electrode surface sufficiently, so that a high power can be supplied without thermal damage of the electrode, improving remarkably deposition rate and homogeneity of the films,
- use high flow rates of carrier gas to remove easily particles generated in the plasma area.

According to Fig. 2, it seems highly probable that their arguments are right.

Resorting to high gas flow rates must present the main advantage to extend the distance needed to establish a parabolic velocity profile and to shift any limitation by diffusion transport. It happens in the work performed by Premkumar et al. (Ref 72), letting us assume that desorption is most often limiting, as already known in thermal CVD processes at atmospheric pressure (Ref 16). Indeed, the length required to establish a parabolic velocity profile is $L_e \approx 0.06 Re \times d$ where Re is the Reynolds number and d the inter-electrode gap. In the case of Ref 72, we find that this length is roughly equal to the length of the DBD. Of course, these assumptions are still to be confirmed, but we have to be very careful at specific effects due to characteristic entrance lengths.

DBD-assisted CVD is mainly used industrially to coat polymers and fabrics, i.e., thermally sensitive materials. Some systems are already used in glass and steel manufacturing. It starts being used commercially in wood industries to ensure protection against mushrooms.

Table 1 List of works performed with low power (<10 W/cm^2) plasma sources for large deposition

Plasma (a)	Precursor	P_{prec}/P_{tot}	React. gas, slm	Flow rate, slm	Temp., °C	Electrical parameters	Distances	Power, W and (P/coated area)	v_d^{max}, µm/h	References
Direct Glow	C_2H_4	0.5%	None	2 (He)	Room temp.			0.3 W/cm^2	2.4	53
Direct DBD	HMDSO HMDSN	<3700 ppm <9100 ppm	O_2 < 3.6 10^5 ppm N_2O < 3.4 10^4 ppm	7-14 (Ar or N_2)	25-400	8-11 kV 5 kHz	G = 1-2 mm		0.76	54
Direct Glow (rotary electrode) (1.8 m/min)	SiH_4	0.1-5%	12.6 (H_2)	1260 (He)	25-200	150 MHz VHF	G = 0.3 mm	300-1000 W (10-35 W/cm^2)	5760	55, 56
Perforated remote (rotating)	DEZn TMAl	25-87 ppm 0.25 ppm	O_2 or CO_2	35.5 (He)	250	13.56 MHz	G = 1.6 mm D = 4 mm	75 (8.8 W/cm^2)	7.2	57-59
Direct (moving)	HMDSO	250 ppm	None	0.03 (He)	Room temp.	1.4-3.2 kV 100-300 kHz	G = 1-1.5 mm	1-4 (~0.08 W/cm^2)	7.2	60
Remote	HMDSO	$T_{bubbler}$ = 22-52 °C	0.25-1 (O_2)	0-1 (Ar)	300-600	4-10 kV 50 Hz	G = 2.5 mm D = 30 mm	40-90	0.6	22
Linear DBD (0.1 m/min)	HMDSO	0.22-1.7%	0-0.2 (O_2)	9 (N_2)	Room temp.	9 kV 40 kHz	G = 1-2 mm	30-35 (0.7 W/cm^2)	6	61
Direct (rotating)	TEOS	$T_{bubbler}$ = 20 °C	0.025 (O_2)	5 (Ar)	25-300	13.56 MHz	G = 3 mm	0-600 (3.4 W/cm^2)	1.7	62
Direct (1.5 m/min)	TEOS	10-200 µL/min	0.1 (O_2)	20 (He)		22 kHz		1000 (0.12 W/cm^2)	4.7	63
Pin-to-plate (0.3 m/min)	PDMS	$T_{bubbler}$ = 20 °C	0.6-1.4 (O_2)	7-15 (He)	<50	5 kV 25 kHz	G = 8.0 mm	260 (1.25 W/cm^2)	1.4	64-67
Direct glow	C_2H_4	0.1-0.5%	None	2-5 (He)		10 kV 0.5-30 kHz	G = 5.0 mm	0.14-0.49 W/cm^2	4.8	68, 69
Direct Glow	HMDSO	$T_{bubbler}$ = 25 °C 0-0.1 (Ar)	None	0-10 (Ar)		5 kV 50 kHz	G = 2.5 mm	15.2 (0.95 W/cm^2)	16.8	70
Direct	HMDSO	1.15 g/h	0-0.1 (O_2) 0-0.1 (NO_2)	1.45 (He)	Room temp.	3-8 kV 40 kHz	G = 1.5-1.7 mm	0-60 (0.625 W/cm^2)	0.72	71
Direct Glow Roll-to-roll	HMDSO	0.4-2.0 g/h	10 (Air)	0.1 (Ar)	Not given	5 kV 130 kHz	G = 0.5 mm	2.3 W/cm^2	25	72

G, inter-electrode gap distance; D, plasma-substrate distance in the remote mode
(a) Substrate velocity when dynamic deposition conditions apply

Peer Reviewed

2.2 High Power Sources

Examples of PECVD works performed with high power sources are shown in Table 2 (Ref 23, 26, 73, 74).

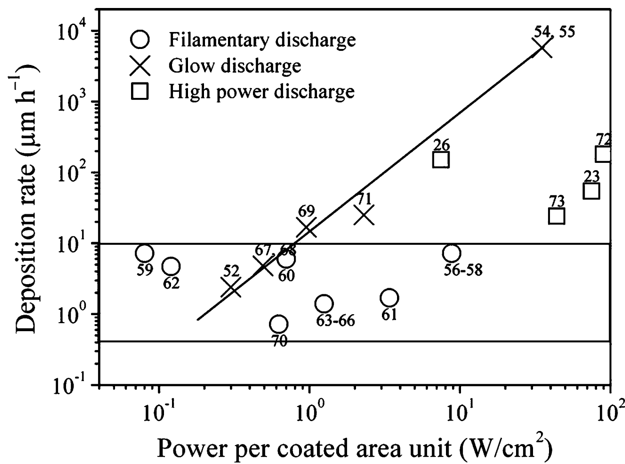

Fig. 2 Maximum deposition rates in studies listed in Table 1 and 2 as a function of the power per coated area unit

Higher injected powers enable high deposition rates. Most of the plasmas are excited by microwave. They are operated in the remote mode to preserve the integrity of the substrate. In this case, CFD codes like Fluent or Comsol are useful to predict at least the flow patterns and to design nozzles that are usually required for an efficient distribution of active species on the surface. The price to pay is a high gas temperature (~1000 K) and an increase in the gas flow rates to control a higher reactivity. Although several efforts have been done to optimize the design of the nozzle, similar injector shapes were proposed (Fig. 3).

The quality of the coatings, in terms of physical or chemical properties, is generally dependent on the deposition rate. The lowest rates lead to thin films with similar properties to those of bulk materials. Desorption of by-products can only be enhanced by a high surface temperature, what is generally incompatible with substrate flowing at high speed under the plasma sources. Depending on industries, process line speed varies from 1 to 100 m/min. Ideally, it should be set to determine the temperature deposition, but such an adjustment is seldom possible. Therefore, it seems difficult to achieve deposition of high quality coatings on cold substrates in continuous flow processes without additional heaters (Ref 54).

Table 2 List of works performed with high power (>10 W/cm^2) plasma sources for large deposition

Plasma	Precursor	P_{prec}/P_{tot}, ppm	React. gas (% total flow rate)	Flow rate, slm	Temp., °C	Power and (*P*/coated area)	v_d^{max}, μm/h	References
Remote μwave	TEOS	500	O_2 or N_2 (30%)	20-50 (Ar)	150	2-15 kW (35-75 W/cm^2)	54	23
Remote μwave	HMDSO	790	O_2 (7%)	70 (Ar)	150-500	0.6-1 kW (5-7.5 W/cm^2)	150	26
Linear arc-jet	TEOS	50	O_2 or N_2 (14%)	10-150 (Ar)	~400	4-30 kW (40-90 W/cm^2)	180	73
Remote μwave	HMDSO	60	None	1-10 (N_2)	Room temp.	2 kW (44 W/cm^2)	24 (estimated)	74

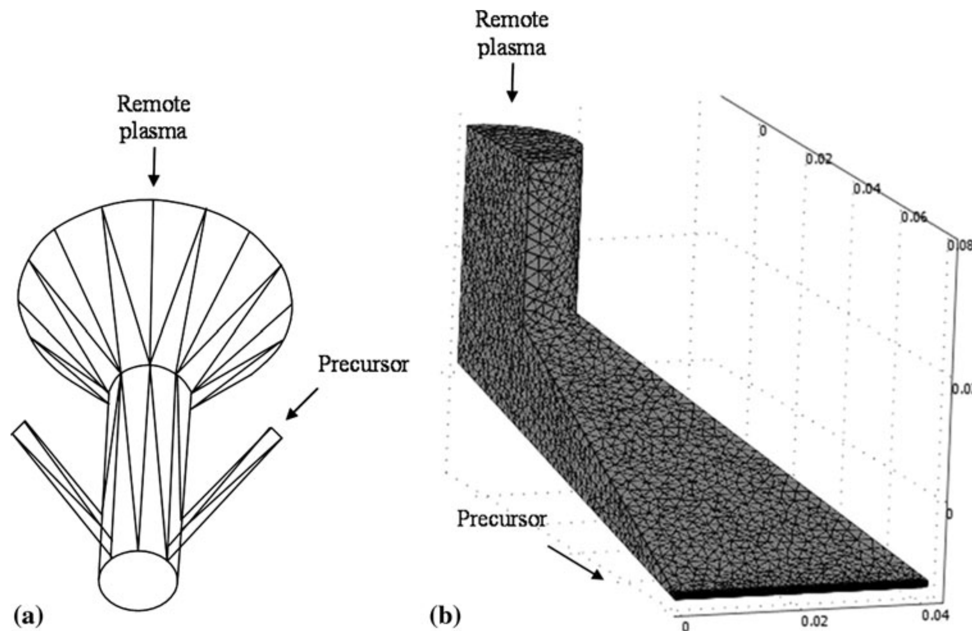

Fig. 3 Example of CFD models of nozzles used in Ref 23 (a) and Ref 26 (b)

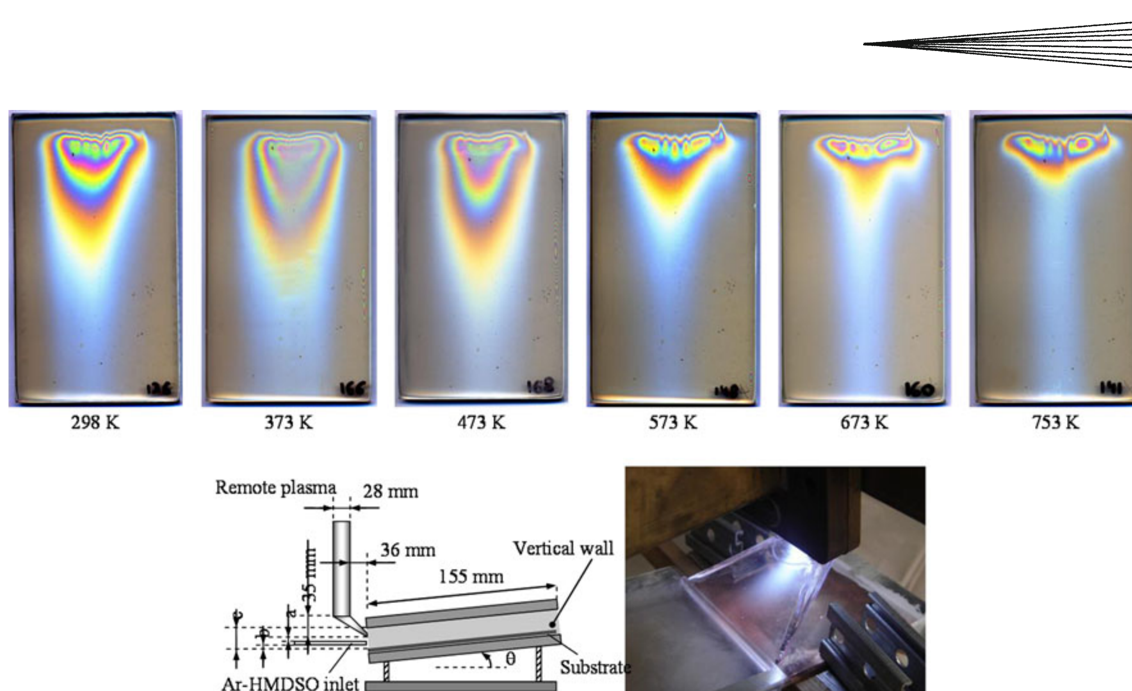

Fig. 4 Picture of coatings deposited at various temperature by chemical vapor deposition enhanced by a remote microwave resonant cavity plasma (see Ref 26 for details). Experimental conditions. Substrate: 6 mm thick glass substrates coated by 3 nm thick TiO_2 layer. HMDSO flow rate: 10 g/h. Topped box. Plasma nozzle height: 2 mm. Plasma power: 800 W. HMDSO carrier gas: 20 slm Ar, plasma mixture: 50 slm Ar and 5 slm O_2, treatment time: 30 s, θ-angle: 20°

Most of thin films deposited by PECVD at atmospheric pressure are silica-like coatings. They are deposited from HMDSO (Hexamethyldisiloxane—$(CH_3)_3$-Si-O-Si-$(CH_3)_3$) and TEOS (TetraEthylOrthoSilicate—$Si(OC_2H_5)_4$) as shown in Table 2. These precursors have ligands containing carbon that has to be removed to get ceramic-like coating. This can be done by ensuring a large amount of atomic oxygen with regards to the precursor. This is achieved either by increasing the power, at least to a certain extent, or by reducing the precursor partial pressure, what decreases the deposition rate. We can also modify the surface temperature.

We show in Fig. 4 an example of thin films deposited at increasing deposition temperature for identical deposition conditions (see Ref 26 for experimental details). We notice that the deposition area drastically changes as temperature rises. Surface reactivity becomes limited to the very beginning of the mixing area between the remote plasma and the precursor flow. Obviously, reactive species no longer reach the surface of the substrate after this area. They react in the gas phase to create powders that are deposited mainly on the center on the substrate where the gas velocity is the highest.

If we look at the Arrhenius plot given in Fig. 5, we notice two regimes. The first one, at low temperature, shows an almost constant deposition rate, corresponding to situations where the surface heating does not affect significantly homogeneous processes in the gas phase.

The second regime, at high temperature, has a positive slope, exhibiting a behavior which is very similar to the so-called feed-rate limiting step in thermal CVD (Ref 75). Powders are created in the gas phase with larger amounts, due to a higher reactivity caused by the surface temperature that affects the gas temperature. Powder synthesis

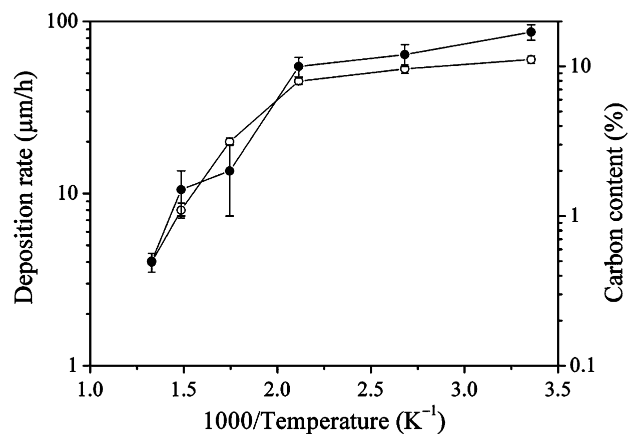

Fig. 5 Arrhenius plot giving the deposition rate as a function of inverse temperature for conditions given in Fig. 4

depletes the gas phase in reactive species beyond the mixing area and limits deposition.

Simultaneously, we notice that the amount of carbon in the coating strictly follows the surface temperature. This result is very similar to that obtained by Hori et al. (Ref 56) who need to heat the coated surface up to about 473 K to significantly improve the quality of their films. A limited surface heating is necessary to enhance species desorption and removal of by-products. However, such a high quality is not always necessary like in the case of adhesion primers deposited from metalorganic compounds.

Finally, confining the gas naturally occurs in dielectric barrier discharges due to the coplanar arrangement of these sources. In remote plasmas, such a confinement is

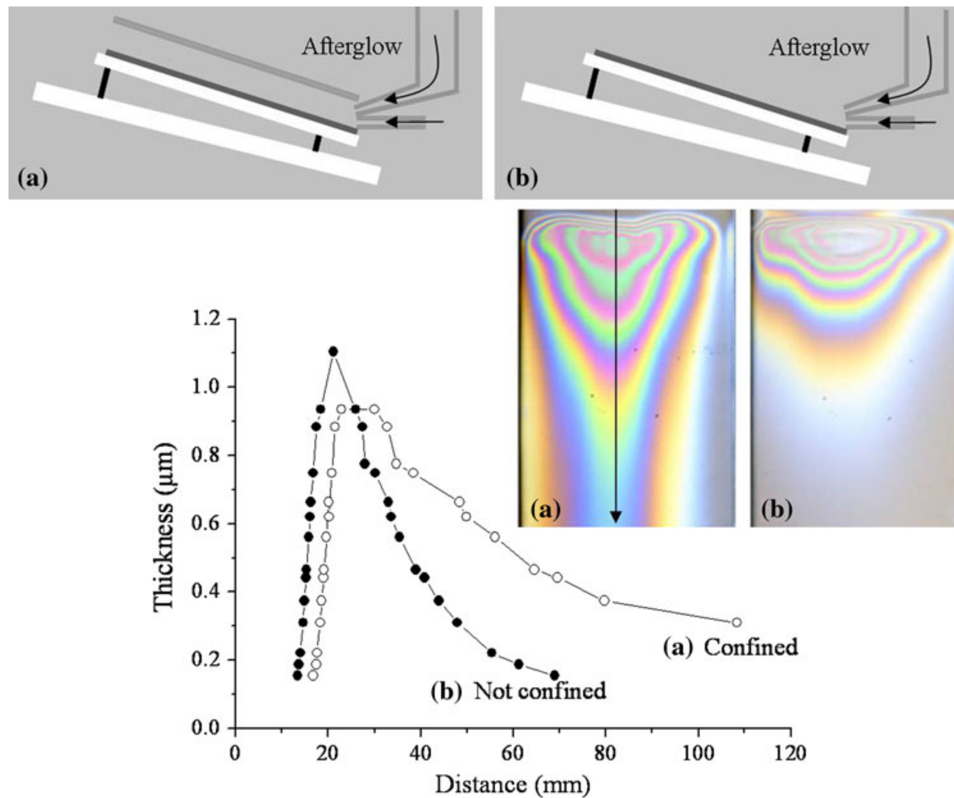

Fig. 6 Influence of the gas confinement on the deposition rate. (a) With confinement. (b) Without confinement. Results obtained by chemical vapor deposition enhanced by a remote microwave resonant cavity plasma (see Ref 26 for details). Experimental conditions. Substrate: 6 mm thick glass substrates coated by 3 nm thick TiO_2 layer. HMDSO flow rate: 40 g/h. Plasma nozzle height: 2 mm. Plasma power: 1000 W. HMDSO carrier gas: 20 slm Ar, plasma mixture: 50 slm Ar and 5 slm O_2, treatment time: 30 s, θ-angle: 24.5°

not ensured a priori. In Fig. 6, we show the influence of confining gases in the remote area by adding one centimeter above the substrate a plate that confines the precursor and the remote plasma flows in a small volume. We notice that the deposition length and the deposition yield are significantly increased. Confining the gas at this scale does not increase the maximum static deposition rate but ensure a better distribution of reactive species and a higher deposition yield, what increases the dynamic deposition rate.

Industrially, these systems are less common than the DBD processes. They are used to produce for instance anti-reflectance coatings on silicon solar wafers.

3. Influence of the Plasma Size on Deposition

Apparently, reducing the size of the plasma sources leads to extremely high deposition rates. We shall distinguish here between plasma jets or torches with millimetric dimension and microplasma with micrometric dimension. The main advantage of these processes, with regards to those described in the previous section, is to localize the deposition over a small area ranging from tens of micrometers in diameter to tens of millimeters. Such processes are particularly promising to treat complex 3D objects by mounting the plasma source on a robot.

3.1 Millimetric Jets and Torches

Table 3 shows a list of works performed with millimetric jets and torches for PECVD at atmospheric pressure (Ref 76-86). Historically, plasma micro-torches were proposed with thermal plasmas (Ref 87-89) rather than with nonequilibrium plasmas. Even though the plasma characteristics are not similar, remote PECVD processes are comparable. Indeed, we notice in Table 3 that almost all processes are operated in the remote mode.

In Fig. 7, we show a set of devices reported in Table 3 and used as microjet or micro-torch to deposit thin films locally at atmospheric pressure. Various excitation modes are used (DC, RF, Microwaves) and several ways to introduce the precursor possible. In Table 3, we observe huge variation of deposition rates. Paradoxically, high power per coated area unit does not always lead to high velocity. In these high temperature plasmas, deposition rates are not simply determined by the injected power. One explanation proposed to justify the rate increase in these highly powered sources is hydrodynamic. At sufficiently high flow rates of plasma gases, the mixing of

Table 3 List of works performed with millimetric torches for localized deposition

Plasma	Characteristic dimensions	Precursor	P_{prec}/P_{tot}	React. gas, slm	Flow rate, slm	Temp., °C	Electrical parameters	Power, W and (*P*/coated area)	v_d^{max}, µm/h	References
Remote DBD	1.6 mm *D* = 17 mm	TEOS	9.2 ppm	0.2 (O_2)	49 (He)	115-350	13.56 MHz	280 W (124 W/cm^2)	6.6	76
Remote DC arc	5.0 mm *D* = 5-20 mm	TEOS	$T_{bubbler}$ = 20 °C	30 (O_2)	1 (He)	150	8.2 kV 23 kHz	300 W (95 W/cm^2)	10.4	77
Remote RF DBD	1.5 mm *D* = 4-13 mm	Zn(acac)$_2$ TTIP	$T_{bubbler}$ = 105 °C $T_{bubbler}$ = 32 °C	(N_2)	(He)	25	13.56 MHz	600 W		78
Direct Glow Nozzle for precursor	15 mm	OMCTS TMCTS	Liquid droplet	0-0.019 (O_2)	1.9 (He)		1.5 kV ac current	Not given	14.6	79
Remote DBD	5 mm *D* = 6 mm	OMCTS	0.05-0.1 g/h	0-0.002 (O_2)	0.2 (Ar)	25-30	13.56 MHz	6 W	0.6-1.2	80
Direct and remote microwave -TIA	3 mm *D* = 0-20 mm	TMS	$T_{bubbler}$ = 7 °C 20-133 ppm	None	15 (Ar)	97	2.45 GHz	450-700 W (700 W/cm^2)	12	81
Remote DBD		TTIP HMDSO			36-43 (Air)		19-23 kHz	Not given	~3000	82
Remote arc girating flow	13 mm *D* = 12 mm	HMDSO TEOS OMCTS	< 2.18 g/min < 0.17 g/min < 0.20 g/min		0.5-5 (He)		19 kHz	700 W		83, 84
Remote DBD	*D* = 18-20 mm	HMDSO TEOS OMCTS	< 2.18 g/min < 0.17 g/min < 0.20 g/min		5 (He)		2.9 kV 22 kHz	300 W		83, 85
Direct plasma (50 mm/s)	15 mm	ZTOMCATS AC8	25 µL/min	None	0.5 (N_2)	Not given	20-30 kV 10-20 kHz	100 W	~300	86
Remote microwave	1 mm *D* = 30-90 mm	HMDSO	0-0.65%	0-0.045 (O_2)	0.225 (Ar)	25-200	2.45 GHz	100 W (2000 W/cm^2)	1500	44, 45

D, plasma-substrate distance in the remote mode

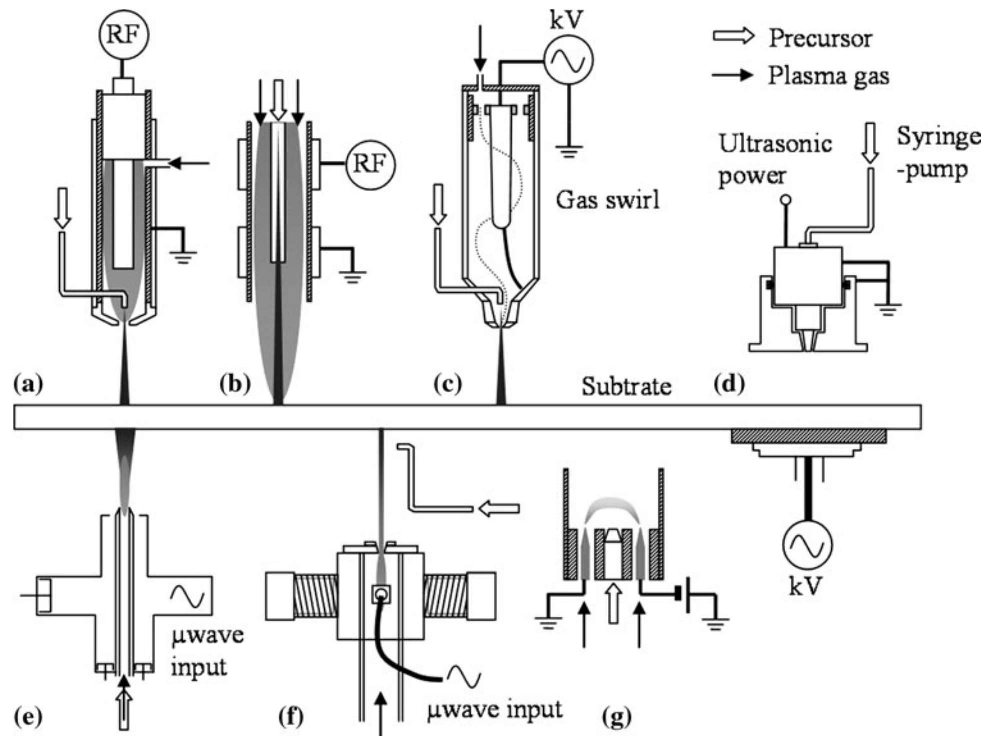

Fig. 7 Principle schematics of millimetric plasma torches used to deposit locally thin films at atmospheric pressure. (a) remote DBD (Ref 76), (b) RF-plasma jet (Ref 80), (c) arc plasma jet (Ref 83-85), (d) DBD with liquid nebulizer (Ref 79), (e) TIA (Ref 81), (f) remote microwave jet (Ref 44, 45), (g) aerosol assisted plasma jet (Ref 86)

reactive species with precursor gases injected in post-discharge is enhanced by a slight turbulent effect (Ref 90). Limited laminar diffusion is compensated by turbulent diffusion that ensures a good mixing of gases. Of course, turbulence must not be too important to limit the development of instabilities and large residence times that lead to powder synthesis.

In Fig. 8, we show the evolution of the deposition rate of thin films deposited by a remote micro-afterglow at atmospheric pressure as a function of the precursor partial pressure in a case where the deposition rate is relatively high (up to 1260 µm/h) (Ref 45). The nonlinear behavior indicates that an intermediary state is created from the HMDSO precursor used in this case. This feature is interesting because it shows that high deposition rate does not necessarily mean a high sticking of the reactive species on the surface and a poorly organized coating.

Consequently, one important aspect deals with the injector of the precursor in the plasma. In Fig. 9, three possibilities are depicted (after Ref 84). Configurations (a) and (c) give deposition profile with Gaussian shape. Configuration (b) may give a torus-like deposition profile, the precursor remaining on the edge of the post-discharge. In Fig. 9(d), we give an example of CFD calculation (after Ref 91) showing the optimization of a flow pattern (configuration shown in Fig. 7a). However, such an optimization process is often quite difficult since nonlinear physical phenomena like thermo-solutal convection have to be included in the hydrodynamic model. This point is extremely important in cases where the molecular masses

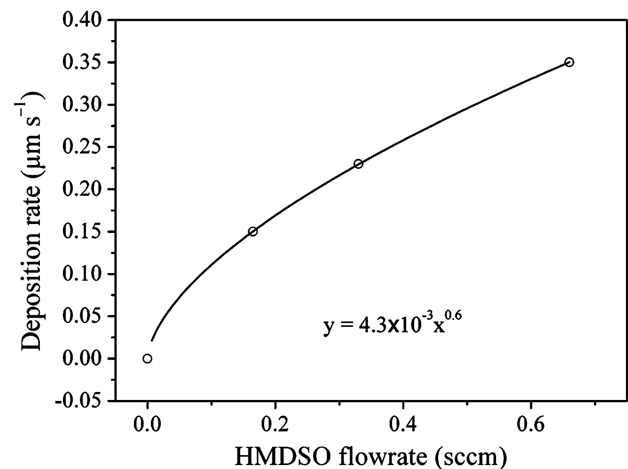

Fig. 8 Evolution of the deposition rate as a function of the HMDSO flow rate in CVD process enhanced by a micro-afterglow (Ref 44, 45). Experimental conditions are as follows. Substrate: 316L stainless steel. Nozzle diameter: 400 µm. Nozzle-substrate distance: 6 mm. Plasma power: 70 W. HMDSO carrier gas: 200 sccm Ar. Plasma gas mixture: 250 sccm Ar and 25 sccm O_2

of the precursors are by far much higher than those of the plasma gases (e.g., a mixture of HMDSO—M = 162.38 g/mol—with H_2). Consequently, the same reasoning applies if we want this time to inert the reaction area and to limit the influence of the ambient atmosphere on the plasma and deposited film properties. If air is the ambient atmosphere, nitrogen and oxygen might be

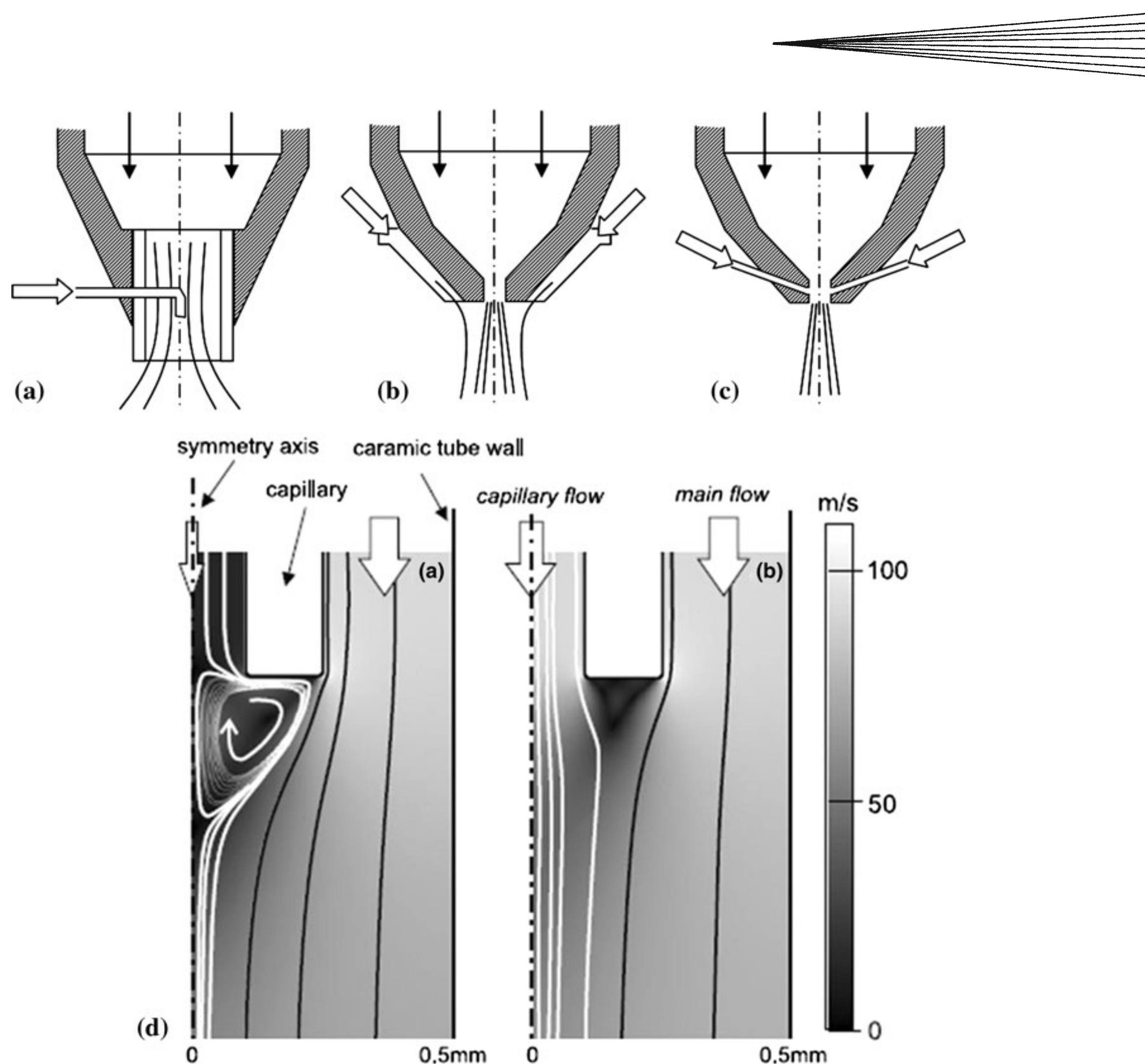

Fig. 9 Possible injection designs to introduce the precursor in the plasma. (a) Injection through a capillary, (b) lateral injection useful also for inerting, (c) Injection through a shower, (d) Example of CFD calculation performed in at low (a) and high (b) flow conditions to optimize the flow injection (after Ref 91). Reproduced with permission from Plasma Phys Control Fusion—IOP

admixed into the plasma and be incorporated into the film. Most processes are inerted by curtains where high nitrogen or argon flows create a protective atmosphere around the jet, preventing the ambient air from reaching the plasma.

Contrary to what was described with DBD systems, in torch-like processes, the gas flow impacts the substrate perpendicularly. For a given flow rate, the distance between the nozzle and the substrate defines the residence time of species in the gas phase. As gas temperature is usually very high (typically 1000 K) due to high powers, deposition processes are basically transient, leading to nonhomogeneous coating composition in depth. Furthermore, the plasma composition changing radially, the coating composition varies also from the center outwards (see Fig. 3 in Ref 80 or Fig. 4 in Ref 81), leading to high stress levels (Ref 45).

The transient nature of these deposition processes may lead to weird effect. For example, the heating of the substrate by the plasma results in increasing the substrate temperature as a function of the processing time, what increases in return the gas temperature. This results in an inverse Arrhenius behavior, decreasing the deposition rate and increasing the rate of powder synthesis in the gas phase (Ref 81).

We also notice in several works (Ref 79, 92, 93), the possibility to resort to liquid precursors. The use of metalorganic compounds is sometimes uneasy. The vapor pressure above the liquid can be extremely low, requiring high temperature to reach sufficiently high partial pressures. Then, direct liquid injection is an interesting alternative to this issue. In this case, liquid electro-spray is preferentially used to create reactive smog of aerosol that reacts chemically with direct or remote plasmas. Although this aspect has not been investigated yet, we assume that it would be interesting to combine PECVD with electro-spinning (Ref 94-96) to create nano-fibers of all kinds.

Microtorches are used industrially to treat torus joints for the automotive industry. These sources are solutions for possible applications requiring local surface treatment.

3.2 Microplasmas

Real chemical vapor deposition with microplasmas is not yet much studied, whereas various deposition processes (reviewed in Ref 29) were proposed to grow deposits locally from microplasmas, like wire evaporation. In this work, we shall concentrate on PECVD processes only as those depicted in Fig. 10. In Table 4, we present works performed in the field of PECVD with micro-discharges (Ref 90, 97-103). We notice that although high deposition rates are obtained, PECVD with micro-discharges did not show yet outstanding capabilities (deposition rates being then close to 240 μm/s) found with similar processes under vacuum, as in the case of the works performed by Abhinandan and Holländer (Ref 46-48).

The input power density to generate the microplasma, and the plasma-substrate distance together with the total flow rate are the most important parameters that affect deposition. Although absolute power delivered to the source is usually small (several watts), it gives extremely high values of power density (up to about 1 MW/cm^3, Ref 98). Depending on the plasma-substrate distance and the total flow rate, the substrate heating may vary a lot. The sensitivity to these parameters is consequently very high and the reproducibility of the deposition process has never been studied. It is certainly a major difficulty to overcome to industrialize this kind of processes. However, the main advantage is to get plasmas very far from the thermodynamic equilibrium and the capability to deposit new materials (Ref 102, 103).

The flow conditions inside the source are critical for the source performance with respect to thin film deposition. If gas velocities of the precursor and discharge species are much different, shear occurs between these two flows, resulting in the formation of vortices (Fig. 9d).

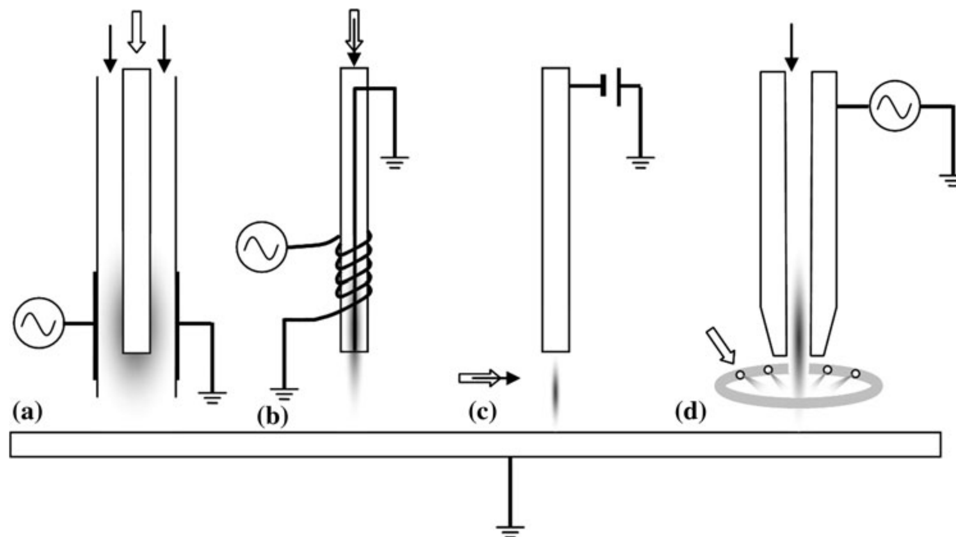

Fig. 10 Principle schematics of micrometric plasma torches used to deposit locally thin films at atmospheric pressure. (a) remote DBD (Ref 91, 97), (b) inductive HF-plasma (Ref 98), (c) DC plasma (Ref 99-102), and (d) RF micro-torch (Ref 103)

Table 4 List of works performed with micro-plasma sources for localized deposition

Plasma	Characteristic dimensions	Precursor	P_{prec}/P_{tot}	React. gas, slm	Flow rate, slm	Temp., °C	Electrical parameters	Power, W and (P/coated area)	v_d^{max}, μm/h	References
RF micro-torch	200 μm D = 1 mm	HMDSO C_2H_2	30-330 ppm 0.03-1%	(0.01) O_2 …	3(Ar) He	25-77	13.56 MHz	5 W (~100 W/cm^2)	3-7	91, 97
UHF micro-torch	100 μm D = 250 μm	CH_4	0.5%	…	0.1 (Ar)	~30	450 MHz	10-30 W (15 kW/cm^2)	120	98
DC glow discharge	100 μm Gap = 400 μm	CH_4	1%	…	0.5 (H_2)	25-300	2-3.8 mA	0.48 A/cm^2	36	99, 100
DC glow discharge	20 μm	CH_4	20-50%	…	0.5 (N_2)	Not given	1-2.5 μA	~0.8 mW (~300 kW/cm^2)	Not given	101, 102
RF micro-torch	700 μm	CH_4	50%	…	0.05 (Ar)	High transient temperature	13.56 MHz	35 W (1.7 kW/cm^2)	Etching	103

D, nozzle-substrate distance

Long residence times cause dust particle formation, inhomogeneous film growth, and deposition inside the source, hence reducing its lifetime.

Glow plasma treatments in capillaries have attracted much attention in the development of novel functional tubes having biocompatibility and hydrophilic or hydrophobic properties (Ref 104-109)

Up to now, no industrial application of these micro-torches in CVD has been developed to our knowledge.

4. Coating Growth and Properties

The growth of coatings influences directly their properties. Depending on the partial pressure of the precursor, powders can be included in the layer (Fig. 11). As in thermal CVD, the supersaturation of the precursor plays an important role on the synthesis of particles in the gas phase and on their possible embedment in the growing layer. Such inclusions are highly detrimental to the film properties.

On the other hand, for a given partial pressure of precursor, the film density evolves as a function of the surface temperature of the substrate. In Fig. 12, we show the influence of the temperature on the growth of a silica-like layer obtained by a remote microwave plasma at atmospheric pressure (Ref 26). Several conclusions can be drawn from these results:

- the growth mode is affected by the temperature. In a recent work (Ref 110), we showed how this growth mode can be controlled not only by the temperature, but also by the carbon content in the film.
- under appropriate temperature conditions, dense films with high-quality can be deposited.
- renucleation may occur at sufficiently high temperature as demonstrated by Fig. 13(a) where surface nuclei are found to be hemispheres over a flat surface and not powders included in the growing film.
- High stress can appear in coatings as shown by the presence of a network of parallel dislocations (Fig. 13b).

Similar observations were drawn in various works (Ref 17, 23, 58). Other important parameters that control the properties of deposited thin films are the level of porosity in the films and the carbon content left from the metalorganic precursor. For example, according to Ref 58, the abrasion resistance of the coating is related to the porosity of the films that depends, in their conditions, on the choice of the precursor (TMDSO or HMDSN).

On the other hand, despite the fact that the substrates can be thoroughly cleaned prior to deposition, adhesion of the coating to the substrate may not always be as high as expected. When particulates such as dust appear to have been incorporated into the coating, these particulates seem to be a source of cracks in the coatings (Ref 23).

Due the transient nature of deposition in roll-to-roll processes, the temperature evolution of the surface flowing under the plasma source makes deposition strongly dependent on heat transfer. One important consequence of this aspect is that deposition, and thus, thin film

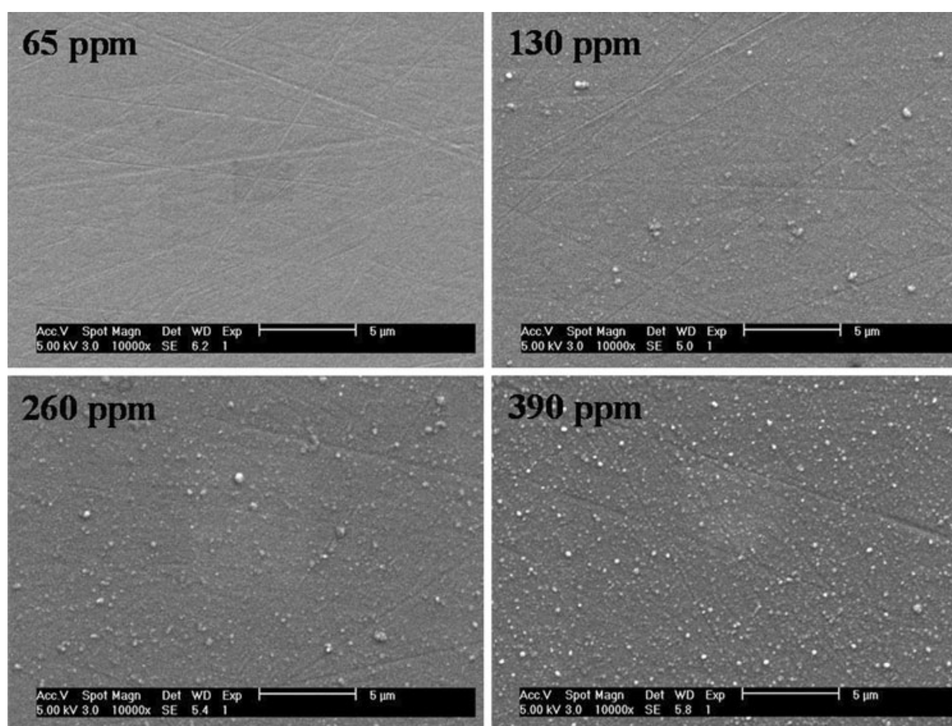

Fig. 11 Top views of silica coatings deposited at various partial pressures of HMDSO. Detailed conditions available in Ref 90

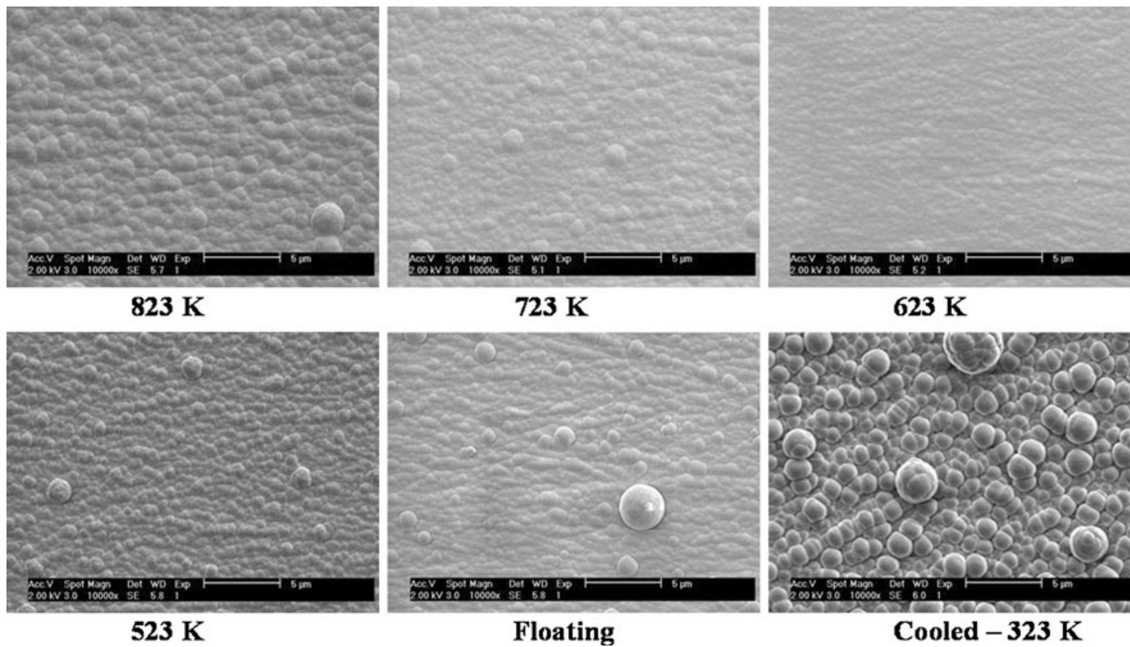

Fig. 12 Influence of the temperature on SiO_2 coatings deposited in a remote microwave plasma. Detailed conditions available in Ref 90

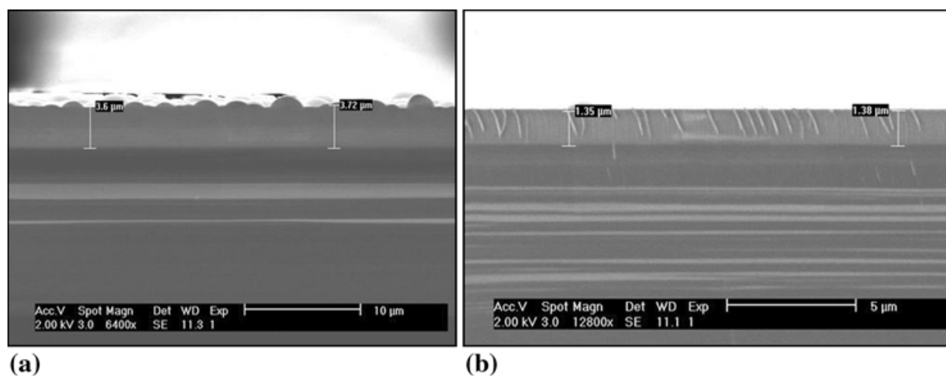

Fig. 13 Cross section views of SiO_2 coatings (same conditions as in Fig. 12). (a): temperature: 823 K. (b) Cooled at 323 K

properties, may depend on the substrate. The deposition rate may vary if deposition is performed on steel or on glass, materials with very different thermal conductivities (Ref 17). Consequently, film composition or density may change sufficiently to affect some properties, like permeability.

5. Conclusion

PECVD at atmospheric pressure is a versatile process that offers a large range of applications.

Concerning sources for coatings on large area, we showed that:

- deposition rates are always below 10 μm/h in filamentary DBD where dissipated power stays below 10 W/cm^2,
- deposition rates in glow discharges are usually higher for the same dissipated power, likely due to mass transport in confined sources. They can reach extremely high values (several mm/h) if high powers (>10 W/cm^2) are applied. Cooling the electrode surface sufficiently and use high speed gas flows of carrier gas are then mandatory,
- in high power sources, gas temperature increases and gas hydrodynamic becomes extremely important to mix active species from the plasma with precursors. Particularly, transient phenomena become important and the correlated time evolution of the gas and surface temperatures may strongly influence the process yield.

When the deposition area decreases, extremely high deposition rates can be obtained (up to about 1 mm/h)

without degrading the film quality. The origin of such a phenomenon is assigned to a slight turbulent effect where diffusion is enhanced without strongly increasing the residence times, avoiding the synthesis of powders. The design of nozzles is then very important. Handling liquid aerosols rather than gaseous precursors seem to be a promising way to deposit a large variety of materials.

In the case of microplasmas, up to now, only few studies were performed. These sources where huge power densities are possible are promising devices to synthesize new materials. However, still much has to be done to control the reproducibility of the treatment conditions.

References

1. E. Mayer and D.E. Shea, Epitaxial Deposition of Silicon Layers by Pyrolysis of Silane, *J. Electrochem. Soc.*, 1964, **111**, p 550-556
2. F.C. Eversteijn, Gas-Phase Decomposition of Silane in a Horizontal Epitaxial Reactor, *Philips Res. Rep.*, 1971, **26**, p 134-144
3. J. Bloem and W.A.P. Claassen, Rate-Determining Reactions and Surface Species in CVD of Silicon: I. The SiH_4-HCl-H_2 System, *J. Cryst. Growth*, 1980, **49**, p 435-444
4. J. Bloem and W.A.P. Claassen, Nucleation and Growth of Silicon Films by Chemical Vapour Deposition, *Philips Tech. Rev.*, 1984, **41**, p 60-69
5. M.L. Hitchman, Heterogeneous Kinetics and Mass Transport in Chemical Vapour. Deposition Processes, *Prog. Cryst. Growth Charact.*, 1981, **4**, p 249-281
6. A.M. Beers and J. Bloem, Temperature Dependence of the Growth Rate of Silicon Prepared Through Chemical Vapor Deposition from Silane, *Appl. Phys. Lett.*, 1982, **41**, p 153-155
7. S. Herrick and D.W. Woodruff, The Homogeneous Nucleation of Condensed Silicon in the Gaseous Si-H-Cl System, *J. Electrochem. Soc.*, 1984, **131**, p 2417-2422
8. M.E. Coltrin, R.J. Kee, and J.A. Miller, A Mathematical Model of Silicon Chemical Vapor Deposition, *J. Electrochem. Soc.*, 1986, **133**, p 1206-1213
9. G. Evans and R. Greif, Effects of Boundary Conditions on the Flow and Heat Transfer in a Rotating Disk Chemical Vapor Deposition Reactor, *Numer. Heat Transfer*, 1987, **12**, p 243-252
10. D.I. Fotiadis and K.F. Jensen, Thermophoresis of Solid Particles in Horizontal Chemical Vapor Deposition Reactors, *J. Cryst. Growth*, 1990, **102**, p 743-761
11. K.F. Jensen and W. Kern, Thermal Chemical Vapor Deposition, *Thin Film Processes II*, J. Vossen and W. Kern, Ed., Academic Press, Orlando, FL, 1991, p 283
12. H. Van Santen, C.R. Kleijn, and H.E.A. Van Den Akker, Mixed Convection in Radial Flow Between Horizontal Plates—I. Numerical Simulations, *Int. J. Heat Mass Transf*, 2000, **43**(9), p 1523-1535 (See also: Mixed Convection in Radial Flow Between Horizontal Plates—II. Experiments, 2000, **43**(9), p 1537)
13. H. Van Santen, C.R. Kleijn, and H.E.A. Van Den Akker, Symmetry Breaking in a Stagnation-Flow CVD Reactor, *J. Cryst. Growth*, 2000, **212**(1-2), p 311-323
14. M.L. Hitchman, W. Ahmed, S. Shamlian, and M. Tainor, Kinetics and Thermodynamics of Chemical Vapour Deposition (CVD) Processes—A Consideration of the Deposition of Doped Polysilico, *Chemtronics*, 1981, **2**, p 147-154
15. M.E. Coltrin, R.J. Kee, and G.H. Evans, A Mathematical Model of the Fluid Mechanics and Gas-Phase Chemistry in a Rotating Disk Chemical Vapor Deposition Reactor, *J. Electrochem. Soc.*, 1989, **136**, p 819-829
16. B.S. Meyerson, Silicon Epitaxy by Chemical Vapor Deposition, *Chemical Vapor Deposition—Principles and Applications*, M.L. Hitchman and K.F. Jensen, Ed., Academic Press Inc., San Diego, CA, 1993, p 219
17. S.E. Alexandrov and M.L. Hitchman, Chemical Vapor Deposition Enhanced by Atmospheric Pressure Non-thermal Non-equilibrium Plasmas, *Chem. Vap. Depos.*, 2005, **11**, p 457-468
18. U. Cvelbar and M. Mozetič, Behaviour of Oxygen Atoms Near the Surface of Nanostructured Nb_2O_5, *J. Phys. D Appl. Phys.*, 2007, **40**, p 2300-2303
19. U. Cvelbar, K. Ostrikov, I. Levchenko, M. Mozetic, and M.K. Sunkara, Control of Morphology and Nucleation Density of Iron Oxide Nanostructures by Electric Conditions on Iron Surfaces Exposed to Reactive Oxygen Plasmas, *Appl. Phys. Lett.*, 2009, **94**, p 211502
20. U. Cvelbar, K. Ostrikov, and M. Mozetič, Reactive Oxygen Plasma-Enabled Synthesis of Nanostructured CdO: Tailoring Nanostructures Through Plasma-Surface Interactions, *Nanotechnology*, 2008, **19**, p 405605
21. U. Cvelbar, Z. Chen, M.K. Sunkara, and M. Mozetič, Spontaneous Growth of Superstructure-Fe_2O_3 Nanowire and Nanobelt Arrays in Reactive Oxygen Plasma, *Small*, 2008, **4**(10), p 1610
22. S.E. Alexandrov, N. McSporran, and M.L. Hitchman, Remote AP-PECVD of Silicon Dioxide Films from Hexamethyldisiloxane (HMSDO), *Chem. Vap. Depos.*, 2005, **11**, p 481-490
23. V. Hopfe, R. Spitzl, I. Dani, G. Maeder, L. Roch, D. Rogler, B. Leupolt, and B. Schoeneich, Remote Microwave PECVD for Continuous, Wide-Area Coating Under Atmospheric Pressure, *Chem. Vap. Depos.*, 2005, **11**, p 497-509
24. V. Hopfe and D.W. Sheel, Atmospheric-Pressure Plasmas for Wide-Area Thin-Film Deposition and Etching, *Plasma Proc. Polym.*, 2007, **4**, p 253-265
25. V. Hopfe and D.W. Sheel, Atmospheric-Pressure PECVD Coating and Plasma Chemical Etching for Continuous Processing, *IEEE Trans. Plasma Sci.*, 2007, **35**, p 204-214
26. R.P. Cardoso, T. Belmonte, F. Kosior, G. Henrion, and E. Tixhon, High Rate Deposition by Microwave RPECVD at Atmospheric Pressure, *Thin Solid Films*, 2011, doi:10.1016/j.tsf.2011.02.003
27. G. Lucovsky and D.V. Tsu, Plasma Enhanced Chemical Vapor Deposition: Differences Between Direct and Remote Plasma Excitation, *J. Vac. Sci. Technol. A*, 1987, **5**(4), p 2231-2238
28. D. Vollath, Plasma Synthesis of Nanopowders, *J. Nanopart. Res.*, 2008, **10**, p 39-57
29. D. Mariotti and R.M. Sankaran, Microplasmas for Nanomaterials Synthesis, *J. Phys. D Appl. Phys.*, 2010, **43**, p 323001
30. W.-H. Chiang, C. Richmonds, and R.M. Sankaran, Continuous-Flow, Atmospheric-Pressure Microplasmas: A Versatile Source for Metal Nanoparticle Synthesis in the Gas or Liquid Phase, *Plasma Sour. Sci. Technol.*, 2010, **19**, p 034011
31. J.P. Borra, E. Bourgeois, and N. Jidenko, Atmospheric Pressure Plasmas for Aerosols Processes in Materials and Environment, *Eur. Phys. J. Appl. Phys.*, 2009, **47**(2), p 22804
32. E. Bourgeois, N. Jidenko, M. Alonso, and J.P. Borra, DBD as a Post-Discharge Bipolar Ions Source and Selective Ion-Induced Nucleation Versus Ions Polarity, *J. Phys D*, 2009, **42**, p 205202
33. C. Tendero, C. Tixier, P. Tristant, J. Desmaison, and P. Leprince, Atmospheric Pressure Plasmas: A Review, *Spectrochim. Acta B: At. Spectrosc.*, 2006, **61**(1), p 2-30
34. L. Woods and P. Meyers, ''Atmospheric Pressure Chemical Vapor Deposition and Jet Vapor Deposition of CdTe for High Efficiency Thin Film PV Devices'', Final Technical Report, NREL/SR-520-32761, August 2002, 44 pp. http://www.doe.gov/bridge
35. B. Dong, J.M. Bauchire, J.M. Pouvesle, P. Magnier, and D. Hong, Experimental Study of a DBD Surface Discharge for the Active Control of Subsonic Airflow, *J. Phys. D Appl. Phys.*, 2008, **41**, p 155201
36. Z. Cao, J.L. Walsh, and M.G. Kong, Atmospheric Plasma Jet Array in Parallel Electric and Gas Flow Fields for Three-Dimensional Surface Treatment, *Appl. Phys. Lett.*, 2009, **94**, p 021501
37. C. Noël, D. Duday, S. Verdier, P. Choquet, T. Belmonte, and H.-N. Migeon, Interaction of Stearic Acid Deposited on Silicon Samples With Ar/N_2 and Ar/O_2 Atmospheric Pressure Microwave Post-discharges, *Plasma Proc. Polym.*, 2009, **6**(S1), p S187-S192

38. K. Ostrikov and A.B. Murphy, Plasma-Aided Nanofabrication: Where is the Cutting Edge?, *J. Phys. D Appl. Phys.*, 2007, **40**(8), p 2223-2241
39. N. Jiang, S. Fa Qian, L. Wang, and H. Xian Zhang, Localized Material Growth by a Dielectric Barrier Discharge, *Thin Solid Films*, 2001, **390**, p 119-122
40. S.E. Babayan, J.Y. Jeong, V.J. Tu, J. Park, G.S. Selwyn, and R.F. Hicks, Deposition of Silicon Dioxide Films With an Atmospheric-Pressure Plasma Jet, *Plasma Sour. Sci. Technol.*, 1998, **7**, p 286-288
41. Y. Shimizu, A.C. Bose, T. Sasaki, D. Mariotti, K. Kirihara, T. Kodaira, K. Terashima, and N. Koshizaki, Development of Cross-Flow Micro-Nebulizer for Atmospheric Pressure Microplasma Deposition and its Application to Prepare Nano-Carbon Materials from Alcohol, *Trans. Mater. Res. Soc. Jpn.*, 2006, **31**(2), p 463-466
42. Y. Shimizu, T. Sasaki, C. Liang, A.C. Bose, T. Ito, K. Terashima, and N. Koshizaki, Cylindrical Metal Wire Surface Coating with Multiwalled Carbon Nanotubes by an Atmospheric-Pressure Microplasma CVD Technique, *Chem. Vap. Depos.*, 2005, **11**, p 244-249
43. T. Kikuchi, Y. Hasegawa, and H. Shirai, Rf Microplasma Jet at Atmospheric Pressure: Characterization and Application to Thin Film Processing, *J. Phys. D Appl. Phys.*, 2004, **37**, p 537-1543
44. G. Arnoult, R.P. Cardoso, T. Belmonte, and G. Henrion, Flow Transition in a Small Scale Microwave Plasma Jet at Atmospheric Pressure, *Appl. Phys. Lett.*, 2008, **93**, p 191507
45. G. Arnoult, T. Belmonte, and G. Henrion, Self-Organization of SiO_2 Nanodots Deposited by Chemical Vapor Deposition Using an Atmospheric Pressure Remote Microplasma, *Appl. Phys. Lett.*, 2010, **96**, p 101505
46. A. Holländer and L. Abhinandan, Localized Deposition by μ-jet-CVD, *Surf. Coat. Technol.*, 2003, **174-175**, p 1175-1177
47. L. Abhinandan and A. Holländer, Localized Deposition of Hydrocarbon Using Plasma Activated Chemical Vapour Deposition, *Thin Solid Films*, 2004, **457**, p 241-245
48. K. Silmy, A. Holländer, A. Dillmann, and J. Thömel, Micro-Jet Plasma CVD with HMDSO/O_2, *Surf. Coat. Technol.*, 2005, **200**, p 368-371
49. D. Mariotti, A.C. Bose, and K. Ostrikov, Atmospheric-Microplasma-Assisted Nanofabrication: Metal and Metal-Oxide Nanostructures and Nanoarchitectures, *IEEE Trans. Plasma Sci.*, 2009, **37**, p 1027-1036
50. D. Mariotti and K. Ostrikov, Tailoring Microplasma Nanofabrication: From Nanostructures to Nanoarchitectures, *J. Phys. D Appl. Phys.*, 2009, **42**, p 092002
51. T. Nozaki, Y. Kimura, and K. Okazaki, Carbon Nanotubes Deposition in Glow Barrier Discharge Enhanced Catalytic CVD, *J. Phys. D Appl. Phys.*, 2002, **35**, p 2779-2784
52. M. Sĭmor, J. Ráhel, P. Vojtek, M. Cĕrnák, and A. Brablec, Atmospheric-Pressure Diffuse Coplanar Surface Discharge for Surface Treatments, *Appl. Phys. Lett.*, 2002, **81**(15), p 2716-2718
53. N. Gherardi, S. Martin, and F. Massines, A New Approach to SiO_2 Deposit Using a N_2-SiH_4-N_2O Glow Dielectric Barrier-Controlled Discharge at Atmospheric Pressure, *J. Phys. D Appl. Phys.*, 2000, **33**, p L104-L108
54. K. Schmidt-Szalowski, Z. Rzanek-Boroch, J. Sentek, Z. Rymuza, Z. Kusznierewicz, and M. Misiak, Thin Films Deposition from Hexamethyldisiloxane and Hexamethyldisilazane under Dielectric-Barrier Discharge (DBD) Conditions, *Plasma Polym.*, 2000, **5**(3/4), p 173-190
55. H. Kakiuchi, Y. Nakahama, H. Ohmi, K. Yasutake, K. Yoshii, and Y. Mori, Investigation of Deposition Characteristics and Properties of High-Rate Deposited Silicon Nitride Films Prepared by Atmospheric Pressure Plasma Chemical Vapor Deposition, *Thin Solid Films*, 2005, **479**, p 17-23
56. Y. Mori, K. Yoshii, H. Kakiuchi, and K. Yasutake, Atmospheric Pressure Plasma Chemical Vapor Deposition System for High-Rate Deposition of Functional Materials, *Rev. Sci. Instrum.*, 2000, **71**(8), p 3173-3177
57. M.D. Barankin, E. Gonzalez, II, A.M. Ladwig, and R.F. Hicks, Plasma-Enhanced Chemical Vapor Deposition of Zinc Oxide at Atmospheric Pressure and Low Temperature, *Solar Energy Mater. Solar Cells*, 2007, **91**, p 924-930
58. M. Morajev and R.F. Hicks, Atmospheric Plasma Deposition of Coatings Using a Capacitive Discharge Source, *Chem. Vap. Dep.*, 2005, **11**, p 469-476
59. G.R. Nowling, S.E. Babayan, V. Jankovic, and R.F. Hicks, Remote Plasma-Enhanced Chemical Vapour Deposition of Silicon Nitride at Atmospheric Pressure, *Plasma Sour. Sci. Technol.*, 2002, **11**, p 97-103
60. R. Foest, F. Adler, F. Sigeneger, and M. Schmidt, Study of an Atmospheric Pressure Glow Discharge (APG) for Thin Film Deposition, *Surf. Coat. Technol.*, 2003, **163-164**, p 323-330
61. X. Zhu, F. Arefi-Khonsari, C. Petit-Etienne, and M. Tatoulian, Open Air Deposition of SiO_2 Films by an Atmospheric Pressure Line-Shaped Plasma, *Plasma Process. Polym.*, 2005, **2**(5), p 407-413
62. X. Xu, Li Li, S. Wang, L. Zhao, and T. Ye, Deposition of SiO_x Films with a Capacitively-Coupled Plasma at Atmospheric Pressure, *Plasma Sour. Sci. Technol.*, 2007, **16**, p 372-376
63. A. Ramamoorthy, M. Rahman, D.A. Mooney, J.M. Don MacElroy, and D.P. Dowling, Thermal Stability Studies of Atmospheric Plasma Deposited Siloxane Films Deposited on Vycor™ Glass, *Surf. Coat. Technol.*, 2008, **202**, p 4130-4136
64. J.H. Lee, T.T.T. Pham, Y.S. Kim, J.T. Lim, S.J. Kyung, and G.Y. Yeom, Characteristics of SiO_2-Like Thin Film Deposited by Atmospheric-Pressure PECVD Using HMDS-O2-Ar, *J. Electrochem. Soc.*, 2008, **155**(3), p D163-D166
65. J.H. Lee, Y.S. Kim, J.S. Oh, S.J. Kyung, J.T. Lim, and G.Y. Yeom, Characteristics of SiO_x Thin Film Deposited by Atmospheric Pressure Plasma-Enhanced Chemical Vapor Deposition Using PDMS-O_2-He, *J. Electrochem. Soc.*, 2009, **156**(7), p D248-D252
66. Y.S. Kim, J.H. Lee, J.T. Lim, J.B. Park, and G.Y. Yeom, Atmospheric Pressure PECVD of SiO_2 Thin Film at a Low Temperature Using HMDS/O_2/He/Ar, *Thin Solid Films*, 2009, **517**, p 4065-4069
67. E. Gil, J.B. Park, J.S. Oh, and G.Y. Yeom, Characteristics of SiO_x Thin Films Deposited by Atmospheric Pressure Chemical Vapour Deposition as a Function of HMDS/O_2 Flow Rate, *Thin Solid Films*, 2010, **518**, p 6403-6407
68. F. Fanelli, F. Fracassi, and R. d'Agostino, Deposition of Hydrocarbon Films by Means of Helium-Ethylene Fed Glow Dielectric Barrier Discharges, *Plasma Process. Polym.*, 2005, **2**, p 688-694
69. F. Fanelli, G. Di Renzo, F. Fracassi, and R. d'Agostino, Recent Advances in the Atmospheric Pressure PE-CVD of Fluorocarbon Films: Influence of Air and Water Vapour Impurities, *Plasma Process. Polym.*, 2009, **6**, p S503-S507
70. R. Morent, N. De Geyter, T. Jacobs, S. Van Vlierberghe, P. Dubruel, C. Leys, and E. Schacht, Plasma-Polymerization of HMDSO Using an Atmospheric Pressure Dielectric Barrier Discharge, *Plasma Process. Polym.*, 2009, **6**, p S537-S542
71. I. Vinogradov and A. Lunk, Film Deposition in the Dielectric Barrier Discharge at Atmospheric Pressure in He/O_2/HMDSO and He/N_2O/HMDSO Mixtures, *Plasma Process. Polym.*, 2009, **6**, p S514-S518
72. P.A. Premkumar, S.A. Starostin, M. Creatore, H. de Vries, R.M.J. Paffen, P.M. Koenraad, and M.C.M. van de Sanden, Smooth and Self-Similar SiO_2-like Films on Polymers Synthesized in Roll-to-Roll Atmospheric Pressure-PECVD for Gas Diffusion Barrier Applications, *Plasma Process. Polym.*, 2010, **7**, p 635-639
73. V. Hopfe, D. Rogler, G. Maeder, I. Dani, K. Landes, E. Theophile, M. Dzulko, C. Rohrer, and C. Reichhold, Linear Extended Arc-jet CVD-A new PECVD Approach for Continuous Wide Area Coating Under Atmospheric Pressure, *Chem. Vap. Depos.*, 2005, **11**, p 510-522
74. M. Brown, P. Hayes, and P. Prangnell, Characterisation of Thin Silica Films Deposited on Carbon Fibre by an Atmospheric Pressure Non-Equilibrium Plasma (APNEP), *Composites A*, 2002, **33**, p 1403-1408
75. J.G. Eden, Photochemical Vapor Deposition, *Thin Film Processes II*, J. Vossen and W. Kern, Ed., Academic Press, Orlando, FL, 1991, p 443

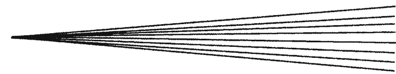

Peer Reviewed

76. S.E. Babayan, J.Y. Jeong, A. Schütze, V.J. Tu, M. Moravej, G.S. Selwyn, and R.F. Hicks, Deposition of Silicon Dioxide Films With a Non-Equilibrium Atmospheric-Pressure Plasma Jet, *Plasma Sour. Sci. Technol.*, 2001, **10**, p 573-578
77. M.H. Han, J.H. Noh, K.W. Park, H.S. Hwang, H.K. Baik, G.H. Doh, I.A. Kang, and S.Y. Lee, *SiO_2 Deposition Using Cold Arc Plasma Jet at Atmospheric Pressure, 28th ICPIG*, Prague, Czech Republic July 15-20, 2007, p 689-690
78. M. Chichina, M. Tichy, P. Kudrna, A. Grinevich, O. Churpita, Z. Hubicka, S. Kment, and J. Olejnicek, A Study of Barrier-Torch Plasma Jet System at Atmospheric Pressure, *Czech. J. Phys. B*, 2006, **56**, p B1212-B1217
79. L.J. Ward, W.C.E. Schofield, J.P.S. Badyal, A.J. Goodwin, and P.J. Merlin, Atmospheric Pressure Glow Discharge Deposition of Polysiloxane and SiOx Films, *Langmuir*, 2003, **19**, p 2110-2114
80. J. Schäfer, R. Foest, A. Quade, A. Ohl, and K.-D. Weltmann, Chemical Composition of SiO_x Films Deposited by an Atmospheric Pressure Plasma Jet (APPJ), *Plasma Proc. Polym.*, 2009, **6**, p S519-S524
81. S.S. Asad, J.-P. Lavoute, C. Dublanche-Tixier, C. Jaoul, C. Chazelas, P. Tristant, and C. Boisse-Laporte, Deposition of Thin SiOx Films by Direct Precursor Injection in Atmospheric Pressure Microwave Torch (TIA), *Plasma Process. Polym.*, 2009, **6**, p S508-S513
82. F. Arefi-Khonsari, J. Pulpytel, S. Bhatt, V. Micheli, and N. Laidani, Deposition of SiO_x and TiO_2 Coatings by an Open Air Non-Equilibrium Atmospheric Pressure Plasma Jet, *Plasma Surface Engineering Conference, Garmisch-Partenkirchen, Germany. Session 13: Atmospheric Plasma Processing, Plasma Spraying*, September 15, 2010, OR1301
83. P. Bringmann, O. Rohr, F.J. Gammel, and I. Jansen, Atmospheric Pressure Plasma Deposition of Adhesion Promotion Layers on Aluminium, *Plasma Process. Polym.*, 2009, **6**, p S496-S502
84. P. Förnsel, C. Buske, U. Hartmann, A. Baalmann, G. Ellinghorst, and K. Vissing, Method and Device for Plasma Coating Surfaces, Invs, United States Patent, US6,800,336B1, 2004
85. J. Kedzierski, J. Engemann, M. Teschke, and D. Korzec, Atmospheric Plasma Jets for 2D and 3D Materials Processing, *Sol. State Phenom.*, 2005, **107**, p 119-124
86. J. Albaugh, C. O'Sullivan, and L. O'Neill, Controlling Deposition Rates in an Atmospheric Pressure Plasma System, *Surf. Coat. Technol.*, 2008, **203**, p 844-847
87. R.N. Savage and G.M. Hieftje, Development and Characterization of a Miniature Inductively Coupled Plasma Source for Atomic Emission Spectrometry, *Anal. Chem.*, 1979, **51**(3), p 408-413
88. G.M. Hieftje, Mini, Micro, and High-Efficiency Torches for the ICP—Toys or Tools?, *Spectrochim. Acta B*, 1983, **38**(11-12), p 1465-1481
89. B.S. Ross, P. Yang, and G.M. Hieftje, The Investigation of a 13-mm Torch for Use in Inductively Coupled Plasma-Mass Spectrometry, *Appl. Spectrosc.*, 1991, **45**(2), p 190-197
90. R.P. Cardoso, T. Belmonte, G. Henrion, T. Gries, and E. Tixhon, Analysis of Mass Transport in an Atmospheric Pressure Remote Plasma Enhanced Chemical Vapor Deposition Process, *J. Appl. Phys.*, 2010, **107**, p 024909
91. J. Benedikt, V. Raballand, A. Yanguas-Gil, K. Focke, and A. von Keudell, Thin Film Deposition by Means of Atmospheric Pressure Microplasma Jet, *Plasma Phys. Control. Fusion*, 2007, **49**, p B419-B427
92. L. O'Neill, L.-A. O' Hare, S.R. Leadley, and A.G. Goodwin, Atmospheric Pressure Plasma Liquid Deposition—A Novel Route to Barrier Coatings, *Chem. Vap. Depos.*, 2005, **11**, p 477-479
93. D. Vangeneugden, S. Paulussen, O. Goossens, R. Rego, and K. Rose, Aerosol-Assisted Plasma Deposition of Barrier Coatings using Organic-Inorganic Sol-Gel Precursor Systems, *Chem. Vap. Depos.*, 2005, **11**, p 491-496
94. J. Doshi and D.H. Reneker, Electrospinning Process and Applications of Electrospun Fibers, *J. Electrostat.*, 1995, **35**, p 151-160
95. D.H. Reneker and I. Chun, Nanometre Diameter Fibres of Polymer, Produced by Electrospinning, *Nanotechnology*, 1996, **7**, p 216-223
96. D. Li and Y. Xia, Electrospinning of Nanofibers: Reinventing the Wheel?, *Adv. Mater.*, 2004, **16**(14), p 1151-1170
97. V. Raballand, J. Benedikt, S. Hoffmann, M. Zimmermann, and A. von Keudell, Deposition of Silicon Dioxide Films Using an Atmospheric Pressure Microplasma Jet, *J. Appl. Phys.*, 2009, **105**, p 083304
98. Y. Shimizu, T. Sasaki, T. Ito, K. Terashima, and N. Koshizaki, Fabrication of Spherical Carbon via UHF Inductively Coupled Microplasma CVD, *J. Phys. D Appl. Phys.*, 2003, **36**, p 2940-2944
99. B. Farouk, D. Staack, T. Farouk, A. Gutsol, and A. Fridman, Atmospheric-Pressure Plasma Microdischarges for High-Rate Deposition, *Proceedings of the International Conference on Mechanical Engineering 2007 (ICME2007)*, December 29-31, 2007, Dhaka, Bangladesh. 12 pp
100. D. Staack, B. Farouk, A. Gutsol, and A. Fridman, Thin Film Deposition using Atmospheric Pressure Microplasmas, *IEEE 34th International Conference on Plasma Science, ICOPS* 2007, p 833
101. T. Ito, K. Katahira, A. Asahara, S.A. Kulinich, and K. Terashima, Carbon System Syntheses on a Chip by Multiple Microplasma CVD, *Sci. Technol. Adv. Mater.*, 2003, **4**, p 559-564
102. T. Ito and K. Terashima, Multiple Microscale Plasma CVD Apparatuses on a Substrate, *Thin Solid Films*, 2001, **390**, p 234-236
103. Z. Yang, H. Shirai, T. Kobayashi, and Y. Hasegawa, Synthesis of Si Nanocones Using rf Microplasma at Atmospheric Pressure, *Thin Solid Films*, 2007, **515**, p 4153-4158
104. H. Yoshiki, K. Abe, and T. Mitsui, SiO_2 Thin Film Deposition on the Inner Surface of a poly (tetra-fluoroethylene) Narrow Tube by Atmospheric-Pressure Glow Microplasma, *Thin Solid Films*, 2006, **515**(4), p 1394-1399
105. C. Penache, C. Gessner, T. Betker, V. Bartels, A. Hollaender, and C.-P. Klages, Plasma Printing: Patterned Surface Functionalisation and Coating at Atmospheric Pressure, *Nanobiotechnol. IEE Proc.*, 2004, **151**(4), p 139-144
106. H. Yoshiki and T. Mitsui, TiO_2 Thin Film Coating on a Capillary Inner Surface Using Atmospheric-Pressure Microplasma, *Surf. Coat. Technol.*, 2008, **202**, p 5266-5270
107. H. Yoshiki, Thin Film Coatings on Capillary Inner Walls by Microplasma, *Vacuum*, 2010, **84**, p 559-563
108. H. Yoshiki, T. Mitsui, T. Sato, T. Morinaga, and S. Marukane, SiO_2 Film Deposition ontThe Inner Wall of a Narrow Polymer Tube by a Capacitively Coupled Microplasma, *Thin Solid Films*, 2010, **518**, p 3526-3530
109. R. Pothiraja, N. Bibinov, and P. Awakowicz, Pulsed Corona Plasma Source Characterization for Film Deposition on the Inner Surface of Tubes, *J. Phys. D Appl. Phys.*, 2010, **43**, p 495201
110. G. Arnoult, T. Belmonte, F. Kosior, M. Dossot, and G. Henrion, On the origin of Self-Organization of SiO_2 Nanodots Deposited by CVD Enhanced by Atmospheric Pressure Remote Microplasma, *J. Phys. D*, 2011 (accepted)